The effect of the a double coating layer–oxide phase ($NiFe_2O_4$) combined with perovskite phase ($La_{0.6}Sr_{0.4}CoO_3$) on a ferritic stainless steel

Diego Afonso da Silva Lima, Gustavo Alberto Ludwig, Matias de Angelis Korb, Alexander Bevian, Célia de Fraga Malfatti
LAPEC – Laboratory of Corrosion Research
PPGE3M
Federal University of Rio Grande do Sul, Brazil

Summary

With the operating temperature reduction of the cells to an intermediate temperature (600°C to 800°C), alloys such as ferritic stainless steel AISI 430 are being used, however for this metal to be used, protective ceramic coatings have been proposed. In this context, in order to protect against oxidation at high temperatures of ferritic stainless steel AISI 430 for application as interconnects in ITSOFC, the present work aimed to at the combination of bilayer coatings obtained by deposition of oxide perovskite (La0.6Sr0. 4CoO3) on the coating of oxide spinel (NiFe2O4). The results showed that the combination of oxide coatings combined with the spinel type oxide of the perovskite tends to prevent degradation of the perovskite, which is usually caused by the migration of the chromium coating creating unwanted phases.

1 Introduction

Fuel cells are appliances that convert chemical energy into electrical energy without combustion, with greater efficiency and fewer pollutants than the currently available equipment [1]. However, for practical applications, it is necessary to increase the strength of these appliances so multiple cells are connected in series to form a stack. This connection from one cell to another is made by means of an interconnection that connects the anode of one cell with the cathode of the adjacent cell [2]. In these operating conditions, the interconnectors are conventionally manufactured of ceramic materials [3], for example, lanthanum chromite ($LaCrO_3$) [4]. However, the replacement of ceramic materials for metallic materials provides a reduction of manufacturing cost [5], improved mechanical strength and coefficient of thermal expansion compatible with other elements, higher electrical and thermal conductivity, and ease of manufacturing to complex geometries [6]. In this context, Intermediate Temperature Solid Oxide Fuel Cells (ITSOFC), which operate at temperatures ranging from 600°C to 800°C allow the use of ferritic stainless steels such as AISI 430 interconnectors. However, they encounter some problems, such as the forming of a layer of chromium (Cr_2O_3), the increase in electrical resistance and volatilization of chromium oxide, and the impairing of the functioning of the appliance [7]. Therefore, in order to make the use of such material possible in the manufacturing of interconnectors, it is necessary to change the composition

of the alloy or the application of surface coatings [8] for protection against oxidation. In this context, perovskite type ceramic coatings have been used for protection against oxidation of ferritic stainless steels at high temperatures. However, as reported in the literature, such coatings at high temperatures undergo degradation due to the diffusion of the element chromium stainless steel substrate into the coating, which can form other oxides, for example, $SrCrO_4$, with low electrical conductivity [9,10]. However, the perovskite type oxides are effective barriers against the diffusion of oxygen into the substrate [11]. Other authors [1,12,13] proposed jackets spinel type oxides, such as $NiFe_2O_4$, which improved electrical performance and form a barrier to volatilization of chromium, but otherwise do not prevent the diffusion of oxygen toward the middle the substrate [2,14]. The main techniques used for obtaining the NiFe and coatings based on La, Sr and Co are: chemical vapour deposition [15], pulsed laser deposition [16], plasma spraying, screen printing and slurry coating, sputtering, spray pyrolysis [6,17,18] and electrodeposited [19,20,21]. Among the deposition techniques presented, the spray pyrolysis has advantages such as the possibility of obtaining coatings with different thicknesses, its low cost and its versatility [18]. In this context, the objective is to get a double-layer coating comprising a first layer of NiFe-based coating obtained by the electrodeposition technique, and a second layer to the base of La, Sr and Co, obtained by the technique of spray pyrolysis. The desired phases of spinel type ($NiFe_2O_4$) oxide and the perovskite type ($La_{0.6}Sr_{0.4}CoO_3$) oxide were obtained after conducting intercalated thermal treatment or at the end of the two depositions. The coatings obtained were characterized for morphology by scanning electron microscopy (SEM), and chemical composition (EDS) and on the structure by diffraction (XRD) X-rays.

2 Materials and methods

2.1 Obtaining the coatings

The ferritic stainless steel AISI 430 was used as the metal substrate, its chemical composition is shown in Table 1 (newsletter of the supplier). The samples were cut in dimensions 20x20x1 mm and sanded until # 1200, and subsequently cleaned for 10 minutes in an acetone ultrasound bath.

Table 1. Chemical composition of the ferritic stell substrate (wt.%).

Cr	C	Si	Mn	Mo	Ni	Co	Al	Nb	Fe
16.03	0.05	0.32	0.4	0.01	0.26	0.018	0.001	0.02	Bal.

In order to obtain a two-layer coating, firstly a NiFe coating was deposited by the electrodeposition technique. The composition of the used electrolyte for electrodeposition and the used parameters in the process are shown in Table 2. Nickel sheets were used as the anode.

Table 2. Solution composition and used electrodeposition parameters for obtaining the NiFe coating.

Solution Concentration / ($g.L^{-1}$)	Deposition parameters by electrodeposition

$NiSO_4$. $6H_2O$	$NiCl_2$. $6H_2O$	H_3BO_3	$FeSO_4$. $7H_2O$	pH	Temperature °C	Current density $mA.cm^{-2}$	Time (hours)
40	5	10	20	2,5	60	5.5	1

The second coating layer was obtained by the spray pyrolysis technique from the precursor solution with nitrates molar ratios of La, Sr and Co (0.6:0.4:1.0) using water as the solvent and propylene glycol (4:5). In Table 3, the operational parameters for the spray pyrolysis technique are presented.

Table 3. Parameters used in the spray pyrolysis process to obtain the La, Sr and Co based coating.

Deposition parameters			
Temperature °C	Substrate distance / cm	Pressure KPa	Deposition Time/min
550	20	294.2	30

For creating the desired phases, spinel ($NiFe_2O_4$) in the first layer and perovskite ($La_{0.6}Sr_{0.4}CoO_3$) in the second layer, heat treatment was performed at a temperature of 800 °C for 2 hours with a heating rate of 5 °C min^{-1}. Three systems were prepared with different combinations of heat treatment, system 1 has not undergone heat treatment, while system 2 has undergone one period of heat treatment after the deposition of the two layers. System 3 received intermediate thermal treatment between the applications of the two layers.

2.4 Characterization of coatings

The surface morphology and evaluation of the cross-sections of the coatings were analyzed by a scanning electron microscopy (SEM) on a Jeol JSM 6510LV microscope, using a voltage of 20 kV. To measure thickness "Image J" software was used and the average values were obtained by measuring 10 points over the cross-sectional images of each of the coating samples. The mapping of the chemical composition of the coatings was performed by energy dispersive spectroscopy (EDS) on a Jeol JSM 6510LV microscope. The structural characterization of the double layer coating was analyzed by X-ray diffraction (XRD) (Philips Analytical X-Ray System Equipment X'Pert-MPD), using the Ka radiation in copper tube under the conditions of 40kV and 25mA using a 0.05 ° step in a 20-70 ° range. This characterization was also performed on the substrate of AISI 430 uncoated stainless steel.

3 Results and discussion

The obtained coating system 1 (Figure 1a), showed a uniform, dense and adherent surface on the substrate of ferritic stainless steel AISI 430, indicating that after the deposition, without thermal treatment, the coatings have good compatibility with each other. However, for system 2 (Figure 1b), which corresponds to the system that has undergone heat treatment in a single period after the deposition of the two coatings, it is possible to observe a cracked

coating. Probably due to the contraction of the first layer (spinel), which tensed the second layer (coating of perovskite), causing cracks in the coating. As observed in Table 4, after the heat treatment process to system 2, both coatings had a reduction on the layer thickness ranging from 32% to 50%, for the electrodeposited coating and for the coating deposited by spray pyrolysis, respectively, which may have contributed to the formation of cracks observed in the coating obtained by the system 2 (Figure 1b). The coating obtained by the system 3 (Figure 1c) presented a uniform, adherent and dense surface. As can be seen in Table 4, the coating undergoes a significant NiFe shrinkage after heat treatment in the range of 70 % to form the spinel type oxide ($NiFe_2O_4$), while the base coating La, Sr and Co, hardly suffers contraction for the formation of the perovskite oxide ($La_{0.6}Sr_{0.4}CoO_3$), thus the intermediate heat treatment prevented the formation of cracks in the coating. The presence of particles observed on the surface of all systems may be due to the temperature deposition technique used in the spray pyrolysis. The high temperature of the substrate during the deposition process may result in a dense morphology with incorporation of particles [20].

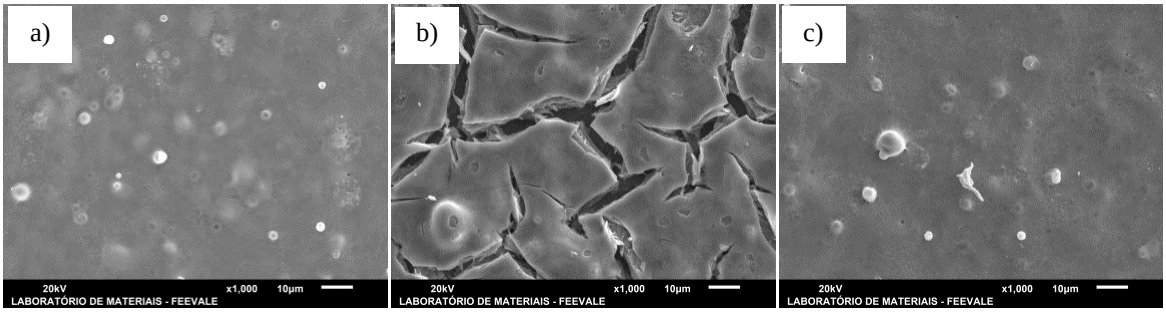

Figure 1. SEM top: a) system1 – without heat treatment, b) system2 – heat treated once after deposition e c) system3 – heat treated after each deposition.

In the diffractogram pattern obtained for the substrate (Figure 2d), as expected, only peaks of FeCr are observed (PDF Number 00-034-0396), belonging to the own ferritic stainless steel substrate. For system 1 (Figure 2c), it is possible to observe the characteristic peaks of NiFe (PDF Number 00-003-1185), corresponding to the coating as deposited, i.e. before the formation of spinel oxide as obtained by the electrodeposition technique (Figure 2c). The second layer to the base of La, Sr and Co obtained by spray pyrolysis does not appear before the heat treatment in the amorphous diffractogram (Figure 2c). System 2 (Figure 2b) revealed the presence of the expected spinel ($NiFe_2O_4$) (PDF Number 00-003-0875) and perovskite ($La_{0.6}Sr_{0.4}CoO_3$) (PDF Number 01-089-5719) oxides. However, it is possible to detect the most intense signal of the phase of the perovskite oxide ($La_{0.6}Sr_{0.4}CoO_3$) in relation to the phase of $NiFe_2O_4$ spinel type oxide. This was possibly due to the effect of the coating thickness of perovskite (who was in the order of 3.79 µm), hindering the detection of the phase spinel ($NiFe_2O_4$). System 3 (Figure 2a), in which the heat treatment was performed after each deposition, evidenced the formation of the spinel type ($NiFe_2O_4$) oxide. Even if the signal has become less intense in comparison to the signal of the perovskite type ($La_{0.6}Sr_{0.4}CoO_3$). This possibly occurred again due to the thickness of the perovskite layer (7.92 µm), that is

over the layer of spinel ($NiFe_2O_4$), making it difficult to detect (XRD). The presence of iron oxides is also observed (Fe_2O_3, PDF Number 01-084-0311) and (Fe_3O_4, PDF Number 00-028-0491). According to some authors, the ferric oxide with the spinel acts as a barrier to volatilization of chromium and improves electrical conductivity [1,22].

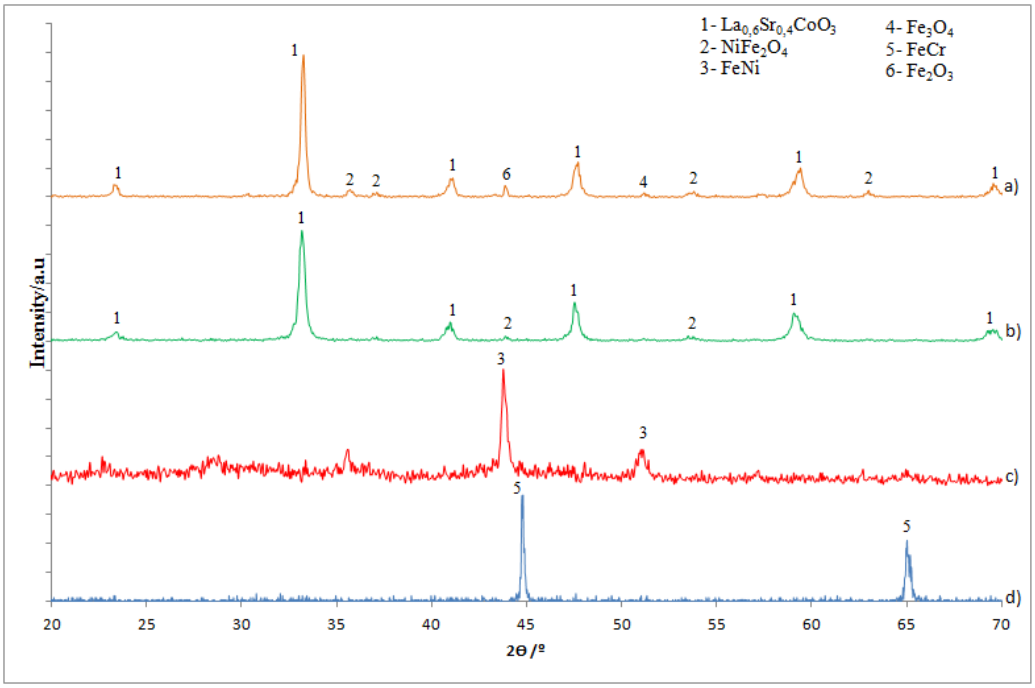

Figure 2. X-ray diffraction, a) system 3, b) system 2, c) system 1 and d) substrate.

The layer thicknesses obtained by the analysis of the images shown in Figure 3, Figure 4 and Figure 5 are presented in Table 4. The thickness of the coatings obtained both after deposition and without heat treatment of system 1 can be observed (Table 4) (NiFe-based and La, Sr and Co). For system 2 (Table 4), the thickness of the electrodeposited coating contracted 32 %, while for the coating obtained by spray pyrolysis contracted 50 %, as mentioned above. However, for system 3, which was subjected to heat treatment after each deposition, only the contraction of the electrodeposited coating NiFe (70 %) for the formation of the spinel type ($NiFe_2O_4$) oxide was noted, since the formation of the spinel oxide was performed prior to spray pyrolysis deposition of the second layer to the base of La, Sr and Co.

Table 4. Layer thicknesses for the obtained system.

System	Coatings	Medium Thickness of the Coating (μm)	Standard Deviation (σ)
System1	Coating 1 (electrodeposition)	3.76	±0.23
	Coating 2 (spray pyrolysis)	7.55	±0.52
System 2	Coating 1 (electrodeposition)	2.55	±0.15
	Coating 2 (spray pyrolysis)	3.79	±0.43

System 3	Coating 1 (electrodeposition)	1.11	±0.20
	Coating 2 (spray pyrolysis)	7.92	±0.56

In Figure 3 the linear mapping by EDS for system 1 can be observed, this characterization is essential to identify the deposition of the second layer to the base of La, Sr and Co (7 to 13.5 µm), which appears amorphous (Figure 2c) [23]. It is noted that the chromium component appears only in the metal substrate region (0 to 2.95 µm), as expected, because the coatings do not have Cr in their composition, while the metallic substrate (ferritic stainless steel) has this element on its composition. Still in Figure 3 (0-7.4 µm), it is possible to observe the presence of iron in both the substrate, which is an alloy based on iron, and on the first deposition layer (NiFe alloy), which also shows the presence of nickel (2.95-6.6 µm), which is found exclusively in this layer. Moreover, as it can be observed, the Co signal is of medium intensity in the substrate area, a fact that may be associated with the proximity of Ka energy of the cobalt and iron, the base element of the ferritic stainless steel substrate (Fe Ka = 6,403 keV, Co Ka = 6,930 keV [24].

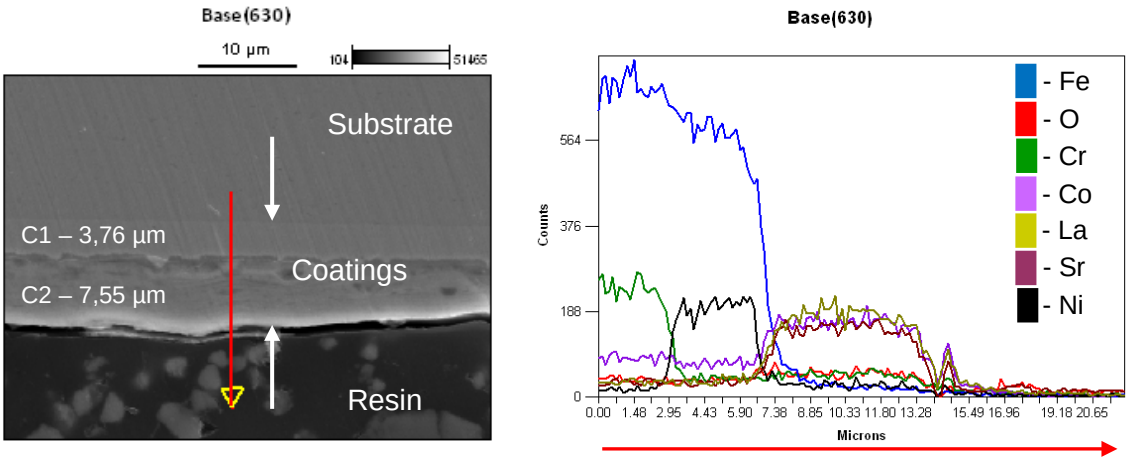

Figure 3. EDS mapping of the cross sectional line scan system 1.

On the linear mapping of system 2 (Figure 4), on the substrate/coating interface it is possible to verify the presence of a chromium-rich region (~ 7 µm), possibly forming a thin layer of chromium (scale) oxide, which is not detected by the X-ray diffraction analysis (Figure 2b), probably due to the thickness of the oxide spinel (2.55 µm) and perovskite (3.79 µm), shown in Table 4 layer. A formation of chromium oxide can be associated with the simultaneous formation process of the spinel and the perovskite oxide because the heat treatment is performed only once after deposition of both coatings. Since the coating to the base of La, Sr and Co is the only barrier to oxygen after crystallization for the $La_{0.6}Sr_{0.4}CoO_3$ phase, and this process occurs at temperatures above 400 °C [23]. However, it is noted that the chrome signal decreases, while on the second layer (perovskite coating), the presence of the element chromium is no longer observed. This shows the characteristic barrier of spinel type ($NiFe_2O_4$) chrome oxide diffusion of the substrate into the coating [2] thus decreasing the

possibility of degradation of perovskite coating by chromium contamination. As it has been reported in the literature, when perovskite oxide coatings are applied directly on a stainless steel substrate and exposed to high temperatures, these coatings suffer degradation due to diffusion of the element chromium of the stainless steel substrate toward the coating, with the possibility of forming other oxides, as, for example, $SrCrO_4$, which has low electrical conductivity [9,10]. The presence of La, Sr and Co on the outermost layer of the coating indicates the formation of the perovskite phase, detected by X-ray diffraction (Figure 2b).

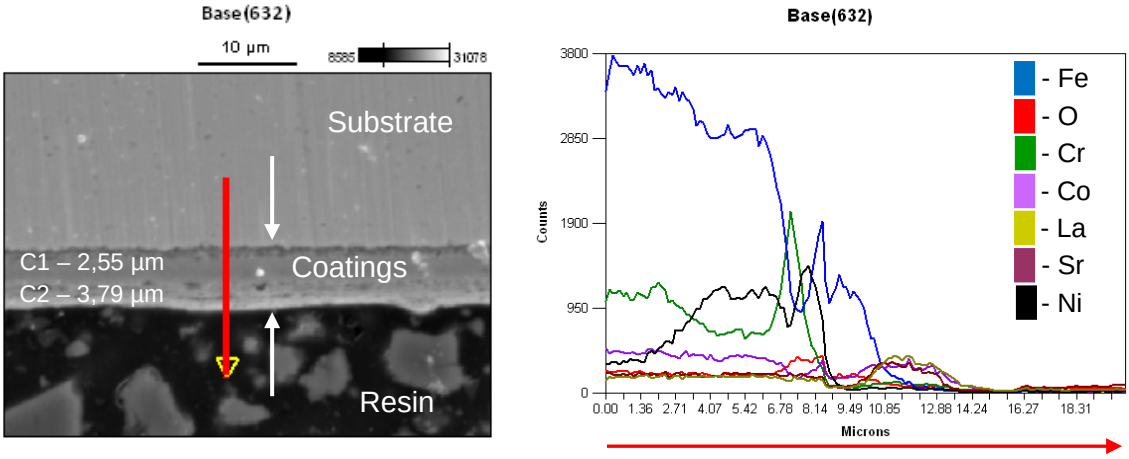

Figure 4. EDS mapping of the cross sectional line scan system 2.

The region of the first deposited layer there are intense signs for the Fe and Ni (8 - 10 µm) elements. This may be related to the formation of the spinel type ($NiFe_2O_4$) oxide, observed by X-ray diffraction (Figure 2). The intense signal of the element nickel in the region of the interface substrate/coating (3 – 6 µm) in Figure 4, is possibly related to the diffusion of nickel from the electroplated NiFe layer toward the substrate. The concentration of nickel in this region may be due to the associated diffusion of same electrodeposited Ni-Fe coating, however, the low diffusion coefficient of nickel in iron [23] prevented the nickel to diffuse faster from the coating to the inside of the substrate, which caused the increase in concentration at the interface between the stainless steel substrate with the coating. On Figure 5, the linear mapping of composition demonstrates the formation of the chromium oxide layer (scale) at the interface between the coating of the spinel type oxide ($NiFe_2O_4$) and the substrate, due to the intense signal in the region of the element chromium. Figure 5, associated with the result of X-ray diffraction (Figure 2a), indicates the presence of the coating of the spinel type ($NiFe_2O_4$) and that this coating, as well as the system 2, possibly prevented the diffusion of chromium into the coating of the perovskite oxide, preventing their degradation by the volatilization of chromium of the stainless steel substrate at elevated temperatures. Moreover, the nickel diffusion is observed once again towards the substrate, as is was already mentioned in the system 2.

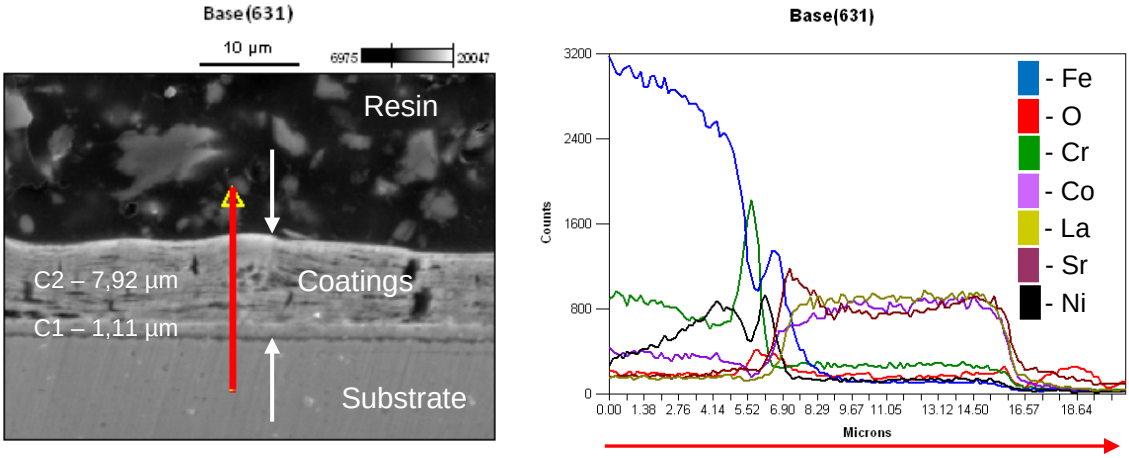

Figure 5. EDS mapping of the cross sectional line scan system 3.

4-CONCLUSIONS

It was possible to get a double layer coating composed of NiFe and La, Sr and Co, deposited on ferritic stainless steel AISI 430, combining, respectively, the techniques of electrodeposition and spray pyrolysis. Moreover, after a heat treatment, it was possible to obtain the oxides of the spinel type ($NiFe_2O_4$) and perovskite ($La_{0.6}Sr_{0.4}CoO_3$).

For the system with thermal treatment performed in one single period after the deposition of NiFe coatings followed by the deposition of the coating to the base of La, Sr and Co, the presence of cracks was observed, possibly due to the contraction of the spinel coating that tensed the coating layer of the perovskite type oxide even during the process of crystallization, since the formation of the phases of the two coatings occur simultaneously. While for system 3, wherein the heat treatment was performed after each deposition, even with the observation of a contraction of the electroplated NiFe layer, there was no cracking of the coating of the perovskite type oxide, because the formation of phases occurred separately, or only after the formation of the spinel phase was deposited on the base layer of La, Sr and Co, followed again by heat treatment.

For the samples after heat treatments, it was evident that the spinel can prevent diffusion of the element chromium for the coating, making it suitable for application as a protective barrier against oxidation of ferritic stainless steel, possibly avoiding the degradation of the coating of perovskite and preventing formation of undesired phases for longer periods of exposure in an oxidising atmosphere. The results indicate that system 3, compared to system 2 studied in this work, is the most suitable for protection as a barrier to ferritic stainless steel used in interconnectors for fuel cells of the solid oxide type of intermediate temperature (ITSOFC).

REFERENCES

[1] Geng S, Li Y, Ma Z, Wang L, Li L, Wang F. Evaluation of electrodeposited Fe–Ni alloy on ferritic stainless steel solid oxide fuel cell Interconnect. J Power Sources 2010;195:3256-60.

[2] Geng S, Qi S, Zhao Q, Zhu S, Wang F. Electroplated NieFe_2O_3 composite coating for solid oxide fuel cell interconnect application. Int J Hydrogen Energy 2012;37:10850-6.
[3] Mekhilefa S, Saidur R, Safari A. Comparative study of different fuel cell technologies. Renew Sust Energ Rev 2012;16:981-9.
[4] Shao Z, Zhou W, Zhu Z. Advanced synthesis of materials for intermediate-temperature solid oxide fuel cells. Prog Mater Sci 2012;57:804-74.
[5] Tucker MC. Progress in metal-supported solid oxide fuel cells: A review. J Power Sources 2010;195:4570-82.
[6] Shaigan N, Qu W, Ivey DG, Chen W. A review of recent progress in coatings, surface modifications and alloy developments for solid oxide fuel cell ferritic stainless steel interconnects. J Power Sources 2010;195:1529-42.
[7] Chatterjee D, Biswas S. Development of chromium barrier coatings for solid oxide fuel cells. Int J Hydrogen Energy 2011;36:4530-9.
[8] Piccardo P, et al. ASR evaluation of different kinds of coatings on a ferritic stainless steel as SOFC interconnects. Surf Coat Technol 2007;202:1221-5.
[9] Korb MA, et al. Modification of the $La_{0.6}Sr_{0.4}CoO_3$ coating deposited on ferritic stainless steel by spray pyrolysis after oxidation in air at high temperature. Int J Hydrogen Energy 2013;38:4760-6.
[10] Chen L, Magdefrau N, Sun E, Yamanis J, Frame D, Burila C. Strontium transport and conductivity of $Mn_{1.5}Co_{1.5}O_4$ coated Haynes 230 and crofer 22 APU under simulated solid oxide fuel cell condition. Solid State Ionics 2011;204-205:111-9.
[11] Yoo J, Woo S-K, Yu JH, Lee S, Park GW. $La_{0.8}Sr_{0.2}MnO_3$ and $(Mn_{1.5}Co_{1.5})O_4$ double layer coated by electrophoretic deposition on Crofer22 APU for SOEC interconnect applications. Int J Hydrogen Energy 2009;34:1542-7.
[12] Geng S, Wang Q, Wang W, Zhu S, Wang F. Sputtered Ni coating on ferritic stainless steel for solid oxide fuel cell interconnect application. Int J Hydrogen Energy 2012;37:916-20.
[13] Xin X, Wang S, Qian J, Lin C, Zhan Z, Wen T. Development of the spinel powder reduction technique for solid oxide fuel cell interconnect coating. Int J Hydrogen Energy 2012;37:471-6.
[14] Kruk A. et al.: Mn–Co spinel protective–conductive coating on AL453 ferritic stainless steel for IT-SOFC interconnect applications. J Solid State Electrochem 2012;17:993-1003.
[15] Fontana S, et al. Metallic interconnects for SOFC: Characterisation of corrosion resistance and conductivity evaluation at operating temperature of differently coated alloys. J Power Sources 2007;171:652-62.
[16] Mikkelsen L, Chen M, Hendriksen PV, Persson A, Pryds N, Rodrigo K. Deposition of $La_{0.8}Sr_{0.2}Cr_{0.9}V_{0.03}O_3$ and $MnCr_2O_4$ thin films on ferritic alloy for solid oxide fuel cell application. Surf Coat Technol 2007;202:1262-6.
[17] Stanislowski M, Froitzheim J, Niewolak L, Quadakkers WJ, Hilpert K, Markus T, Singheiser L. Reduction of chromium vaporization from SOFC interconnectors by highly effective coatings. J Power Sources 2007;164:578-89.

[18] Muecke UP, Luechinger N, Schlagenhauf L, Gauckler LJ. Initial stages of deposition and film formation during spray pyrolysis – Nickel oxide, cerium gadolinium oxide and mixtures thereof. Thin Solid Films 2009;517:1522-9.
[19] Wu J, Gemmen RS, Manivannan A, Liu X. Investigation of Mn/Co coated T441 alloy as SOFC interconnect by on-cell tests. Int J Hydrogen Energy 2011;36:4525-9.
[20] Wei W, Chen W, Ivey DG, Oxidation resistance and electrical properties of anodically electrodeposited Mn–Co oxide coatings for solid oxide fuel cell interconnect applications. J Power Sources 2009;186:428-34.
[21] Tondo E, Boniardi M, Cannoletta D, Riccardisc MF, Bozzini B. Electrodeposition of yttria/cobalt oxide and yttria/gold coatings onto ferritic stainless steel for SOFC interconnects. J Power Sources 2010;195:4772-8.
[22] Qu W, Jia L, Hill JM, Ivey DG. Eletrical and Microstructural Characterization of Spinel Phases as Potential Coatings for SOFC Metallic Interconnects. J Power Sources 2006;153:114-24.
[23] Karageorgakisa NI, Heel A, Hütter AB, Rupp JLM, Graule T, Gauckler LJ. Flame spray deposition of $La_{0.6}Sr_{0.4}CoO_{3-\delta}$ thin films: Microstructural characterization, electrochemical performance and degradation. J Power Sources 2010;195:8152-61.
[24] Iwasawa K, Taniguchi Y. The X-ray Baldwin effect. Astrophys J 1993;413:L15-8.